

## Effect of adding Lanthanum ( $\text{La}^{3+}$ ) on surface performance of Ni-P electroless plating coatings on RB400 support anchor rod steel

Ruizhen Xie<sup>1</sup>, Hongyan Zhang<sup>1</sup>, Jiaojuan Zou<sup>1</sup>, Naiming Lin<sup>1,2,\*</sup>, Yong Ma<sup>1</sup>, Zhenxia Wang<sup>1</sup>, Wei Tian<sup>1,3\*</sup>, Xiaofei Yao<sup>4</sup>, Pengju Han<sup>5</sup>, Zhihua Wang<sup>2</sup>, Bin Tang<sup>1</sup>

<sup>1</sup> Research Institute of Surface Engineering, Taiyuan University of Technology, Taiyuan, 030024, P. R. China

<sup>2</sup> Shanxi Key Laboratory of Material Strength & Structure Impact, Taiyuan University of Technology, Taiyuan, 030024, P. R. China

<sup>3</sup> China United Northwest Institute for Engineering & Research, Xi'an, 710082, P. R. China

<sup>4</sup> School of Materials and Chemical Engineering, Xi'an Technological University, Xi'an, 710032, P. R. China

<sup>5</sup> Department of Civil Engineering, Taiyuan University of Technology, Taiyuan, 030024, P. R. China

\*E-mail: [lnmlz33@126.com](mailto:lnmlz33@126.com), [76134289@qq.com](mailto:76134289@qq.com)

Received: 6 January 2016 / Accepted: 2 March 2016 / Published: 1 April 2016

---

Anchor rod, a common support material in engineering which is often used in civil engineering structures, such as roadway, mines, underground tunnels and rock slope supporting and so on. Owing to the complex service environment and condition, the anchor rod is susceptible to wear and corrosion. In order to improve the wear and corrosion resistance of anchor rod and increase the service lifetime during operation, Ni-P coatings have been prepared on RB400 anchor rod steel via electroless plating. Rare earth element of Lanthanum ( $\text{La}^{3+}$ ) with various concentrations have been added into the electroless plating solution. The surface morphologies, phase constitutions and cross-sectional composition distributions of phosphorus contents in the coatings were characterized by scanning electron microscope (SEM), X-ray diffraction (XRD) and glow discharge optical emission spectroscopy (GDOES). Tribological performance and corrosion resistance of the obtained Ni-P coatings were investigated by reciprocating wear testing machine and electrochemical workstation. The results showed that the  $\text{La}^{3+}$  which played an important role on refining and modifying grain, had significantly influences the properties of Ni-P coatings. In terms of wear resistance, 0.25 g/L is the optimum supplementation, but the effect of  $\text{La}^{3+}$  on the wear resistance is not significant. While the La-coatings with outstanding corrosion resistance exhibit the highest corrosion potential, lowest corrosion current density and maximum resistance value between solution and substrate when the supplementation is 0.50 g/L.

---

**Key words:** electroless plating; anchor rod; Ni-P coating; rare earth; Lanthanum; wear; corrosion

## 1. INTRODUCTION

Anchor rod, a common support material in engineering, is often used in civil engineering structures, such as roadway, mines, underground tunnels and rock slope supporting and so on (see Figure 1). Due to the concealment of underground support engineering[1], the quality of anchor rod plays a vital role in the construction and security. The deterioration of anchor rod occurs in the complex geological and water quality environment and the wear and corrosion is the common failure mode in this situation. It is well known that the failure of engineering materials is mainly determined by the surface properties of the material rather than by its bulk properties. Amongst the surface engineering technologies, electroless plating is an effective method to provide protection and strengthen its performance for variety metal materials[2-4]. Meanwhile it has no special requirements for substrate geometries. Electroless plating is a process that the reduction and constant deposition of metal ions is achieved in liquid solution containing a reducing agent without impressed current.

Malecki, firstly proposed the mechanism of the electroless plating, provided the experience rate equation of plating bath on the basis of exploration to the kinetics processes of the reaction[5]. Up to now, the studies of Ni-P electroless plating on steels have made great progress, especially on different types of steels under various special service environment and the addition of different materials possessing special properties (nanomaterials, rare metals and rare earth elements, etc.). Owing to the largest reserve of rare earth for china, the research and development of rare-earth topics is of great significance. Published work has showed that the supplement of rare earth elements in the conventional binary plating solution can significantly improve the properties of the Ni-P coating[6, 7]. For the electroless plating Ni-P proceeded on Q235 carbon steel in the acid plating bath, appropriate addition of  $\text{La}^{3+}$  had improved the stability of plating bath, the deposition rate and the corrosion resistance of the coating and reduced the plating temperature simultaneously[8, 9]. Ternary Ni-Ce-P coatings on the low-carbon steel plated in an alkaline citrate-bath system presented better corrosion resistance than binary Ni-P plating coatings during the continuous salt spray tests[10]. It was found that adding  $\text{Ce}^{n+}$  ( $n=3, 4$ ) ions could promote the deposition of phosphorus and reduce the coating porosity. Beside the Ni-P/nano- $\text{CeO}_2$  composite coatings on the low carbon steel under acidic condition exhibit the excellent corrosion resistance[11]. While other studies also indicated that excessive addition of rare earth elements (La, Pr and Nd) has negative effects on the deposition rate and corrosion resistance [12, 13].

According to the pH values of the plating solution, electroless nickel plating can be classified into two categories: acidic and alkaline. And in this article the acidic electroless plating solution is the experiment environment. The common acidic electroless plating bath composition is consist of nickel salt (sulphate or chloride salt), reducing agent (sodium hypophosphite or borohydride), complexing agents (acetate, citrate, lactic acid, succinic acid, glycolic acid, etc.), stabilizers (heavy metal salts, thiourea, fluoride, etc.) and pH buffering agents (ammonia water, hydrochloric acid, etc.). In this work  $\text{La}^{3+}$  was added into the traditional binary electroless plating bath aiming to further improve the wear resistance and corrosion resistance of anchor rod.

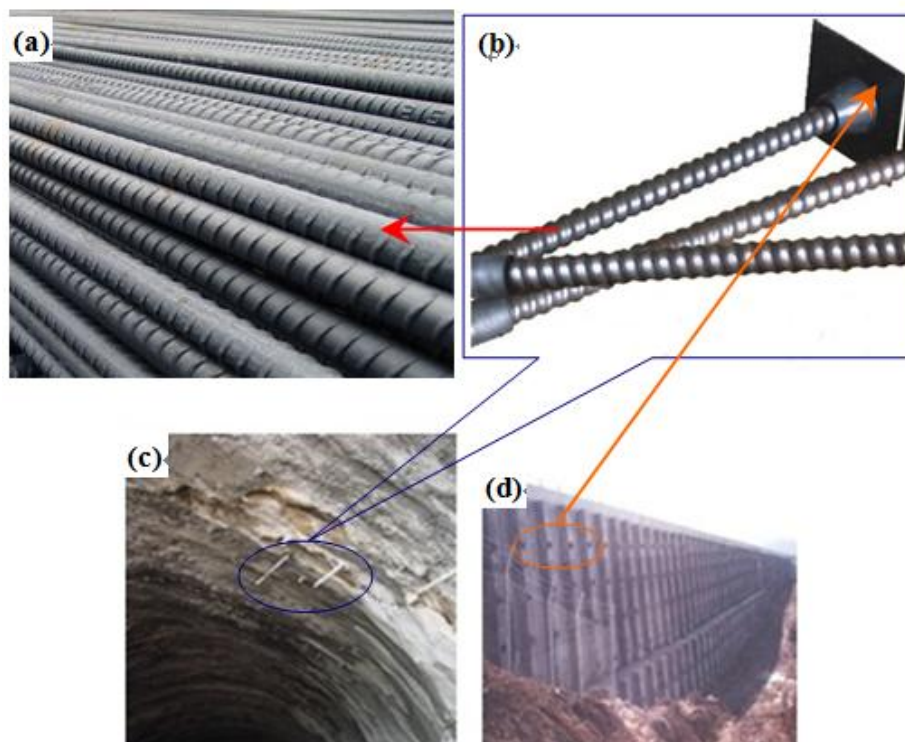


**Figure 1.** Commonly used engineering anchor rod

## 2. EXPERIMENTAL PROCEDURE

Owing to the less experiments and analysis even the presence of some opposite results about La (atomic radius, 0.1877 nm),  $\text{La}^{3+}$  is chosen as the additional element. And the effect of  $\text{La}^{3+}$  on the wear resistance and corrosion resistance and the action mechanisms of  $\text{La}^{3+}$  are studied basing on the basic electroless plating solution and the practical anchor rod material.  $\text{La}^{3+}$  was added in the form of rare earth salt ( $\text{La}(\text{NO}_3)_3$ ) to guarantee uniform dispersion of the solution. Before plating ultrasonic dispersion of the mixed solution (prepared rare earth-nitrate solution + original plating solution) is conducted to insure the uniform and stable of the solution. It is worth noting that the modification of rare earth to the morphology of coating is valid only in a certain extent, so the choice of appropriate addition of it is crucial. The characterization and analysis of the different La-add electroless plating coating is conducted.

### 2.1 Experimental materials and pre-treatment

As a common type of anchor rod, reinforced bar RB400 steel was chosen for the experiments. The chemical composition of RB400 was suggested in Table 1. The samples were cut into a size of  $\Phi 18 \text{ mm} \times 3 \text{ mm}$  as substrate by an electro-spark wire-electrode cutting machine. The surfaces were finely ground on SiC abrasive papers to 1000 grit size, followed by ultrasonic cleaning in acetone bath.

**Table 1.** The chemical composition of RB400 steel

Element	C	Mn	Si	P	S	Fe
Wt.%	0.23	1.42	0.63	0.037	0.033	BAL.

Pre-treatment procedure is as follows:

1. Alkaline cleaning: samples were firstly immersed into the alkaline solution of 85 °C for 5 min to remove the oil. (the formula of the alkaline solution is as shown in Table 2 )

2. Acidic cleaning one: then the samples were washed by 20 vol. % HCl for 1-2 min under ambient temperature to dissolve the rust and the ion remaining on the surface of the samples.

3. Acidic cleaning two: finally the samples were activated by 5 vol. % H<sub>2</sub>SO<sub>4</sub> for 1 min under ambient temperature to form numerous small activity centers, increase the surface activity and facilitate the next deposition process.

It is worth noting that the samples should be rinsed by deionized water after each step to exclude the effect of the previous step on the next step. All pre-treatment procedure is for laying the better foundation of the follow-up plating experiment.

**Table 2** The formula of the alkaline solution

Ingredient	Content(g/L)
sodium hydroxide(NaOH)	70
sodium carbonate(Na <sub>2</sub> CO <sub>3</sub> )	40
sodium phosphate(Na <sub>3</sub> PO <sub>4</sub> )	20
sodium silicate(Na <sub>2</sub> SiO <sub>3</sub> )	10

## 2.2 Electroless plating

Electroless plating solution was prepared according to the formula (Table 3). And the adding order of the components and the pH value (4.5–6.0) adjustment of the plating solution should be paid attention to. Then the plating solution was heated to the desired temperature (85–88 °C) in water bath. Finally, the samples were suspended in the plating solution with certain temperature for 1 h. After the experiment, the samples were taken out and washed with the distilled water to clean the plating solution and other residual impurities on the surface.

**Table 3.** Electroless plating solution formula of adding rare earth experiment

Compound	Concentration (g/L)
Nickel sulfate ( $\text{NiSO}_4 \cdot 6\text{H}_2\text{O}$ )	40
sodium hypophosphite ( $\text{NaH}_2\text{PO}_2 \cdot \text{H}_2\text{O}$ )	25
Sodium citrate ( $\text{Na}_3\text{C}_6\text{H}_5\text{O}_7 \cdot 2\text{H}_2\text{O}$ )	45
Sodium acetate ( $\text{CH}_3\text{COONa} \cdot 3\text{H}_2\text{O}$ )	40
$\text{La}^{3+}$ ( $\text{La}(\text{NO}_3)_3 \cdot 6\text{H}_2\text{O}$ )	0.15, 0.25, 0.5, 0.75

### 2.3 Characterizations and testing

Surface morphologies and phase constitutions of the coatings were characterized by scanning electron microscope (SEM) and X-ray diffraction (XRD). The phosphorus contents of the coatings changing with the depth from the surface was characterized through the glow discharge optical emission spectrometry (GDOES). The microhardness values of the samples were characterized by the HVS-1000A microhardness tester under the load of 50 g with a loading time of 20 s. The corrosion resistance of the coatings with 1 cm<sup>2</sup> effective area in 5 wt. % NaCl solution was tested by three electrode system on electrochemical workstation. Electrochemical measurements of polarization curves (under the potential sweep voltage of -0.5 V~+1.5 V vs. open circuit potentials (OCPs) with a scanning rate of 1 mv/s) and electrochemical impedance spectroscopy (EIS) were conducted. Tribological behaviors of the coatings were tested on the MFT-R4000 reciprocating wear tester against high carbon chrome steel balls ( $\Phi$  5 mm) under the condition of load 5 N for 30 min. Tribological characteristics of the tested samples were defined by comparing the friction coefficients and mass losses. The specimens were thoroughly cleaned with acetone in an ultrasonic bath before and after each test. An analytical balance with an accuracy of 0.01 mg was employed to weigh the original and worn samples.

## 3. RESULTS AND DISCUSSION

### 3.1 Microstructural characterizations

Figure 2 and Figure 3 reveal the morphologies of pure Ni-P coating and the Ni-P-La<sup>3+</sup> coatings respectively. The effect of adding La<sup>3+</sup> on the surface morphology of the Ni-P plating coating is significant[14]. As shown in Figure 2 and Figure 3, it can be seen that the surface cellular particles of the coating were refined and the arrangement were more compact. And the trend was getting more obvious with increasing the addition of La<sup>3+</sup>. When the addition amount of La<sup>3+</sup> was 0.50 g/L, the coating surface was very smooth, and the compact degree of cellular particles was the best. As the concentration of La<sup>3+</sup> was increased to 0.75 g/L, the coating surface become rougher, the cellular particles were significantly bulged. Generally excessive rare earth ions have toxic effects on the efficient deposition of the coating. Due to the continuous coverage of rare earth ions in the interface can reduce the reactivity of hypophosphite and catalytic point, the oxidation reaction of hypophosphite is suppressed and the phenomenon of “poisoning” appears during the entire course of the reaction[8].

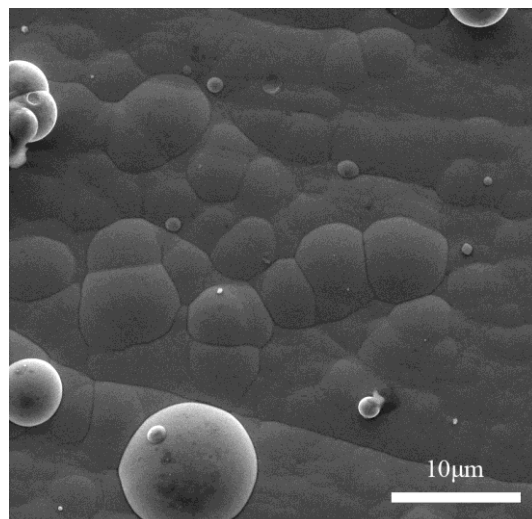


**Figure 2.** Surface morphology of Ni-P coating with magnification of 5000×

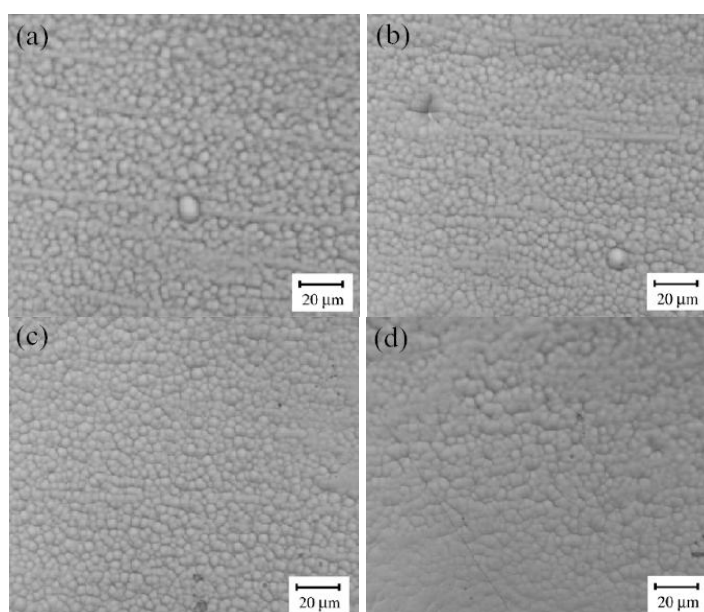


**Figure 3.** The surface topography of electroless Ni-P plating under different concentration of La<sup>3+</sup> (magnification of 1000×): (a) 0.15 g/L ( b) 0.25 g/L ( c) 0.50 g/L ( d) 0.75 g/L

In Figure 4 the peak shape ( $2\theta=45^\circ$ ) is the characteristic peak of (111) crystal face in Nickel crystal. The XRD peaks of the Ni-P coating are diffuse scattering peaks with certain width, which show that the coatings exhibit the characteristic of amorphous diffraction. According to the theory of structural chemistry, electronegativity between transition metals Ni and metalloid elements P has larger difference and the interaction between them is stronger, so the formation of amorphous is very easy. While the FWHM of the peaks for the coatings containing La become narrow and show significant features of microcrystalline diffraction. Rare earth elements with the outstanding adsorption properties reduced the surface activation energy of the substrate, promote the lattice oriented growth of the metal atom along the substrate, reduced the trend of forming amorphous state and refined and

modified the crystal grain[15]. In addition, compared with the XRD patterns of conventional binary coating, the XRD pattern of the coating containing different concentration of  $\text{La}^{3+}$  have fewer small peak, which maybe is caused by the adsorption of different concentration of  $\text{La}^{3+}$  at the growing point on the corresponding crystal face and the coverage of the previously displayed crystal face. It is difficult that the La ions are reduced to the form of metal, so there is no the La in the XRD patterns.

During the electroless nickel, the reduction of nickel ions need the electron provided by oxidation process of hypophosphite, while the special electron shell structure of rare earth elements may provide the vacant orbital for the transportation of the free electron. So the rare earth elements can accelerate the velocity of the electrons and increase the deposition process of metal ions. On the one hand, rare earth elements with strong adsorption capacity can be preferentially adsorbed at the surface defect on the substrate. Then the surface energy is reduced, the nucleation rate and grain density of coating will be increased. The deposition rate and compactness of the coating are increased simultaneously. On the other hand, see from the electrochemical point, the transformation of the electron shell structure (at the interface) caused by the rare earth nitrates hinder the diffusion between the interfaces. So the difficulty of the deposition of Ni atoms is increased and the effect of rare earth ions on the deposition rate is weakened. Besides rare earth ions can precipitate easily in the form of gum hydroxide and a large amount of metal ions will precipitate in the form of a complex compound during the change of pH value in the plating solution. That is to say the reduction deposition of the metal ions is slowed down and the surface quality of the coating is deteriorated. In view of the above, the amount of rare earth elements should not be excessive, otherwise the opposite effect will be acquired.

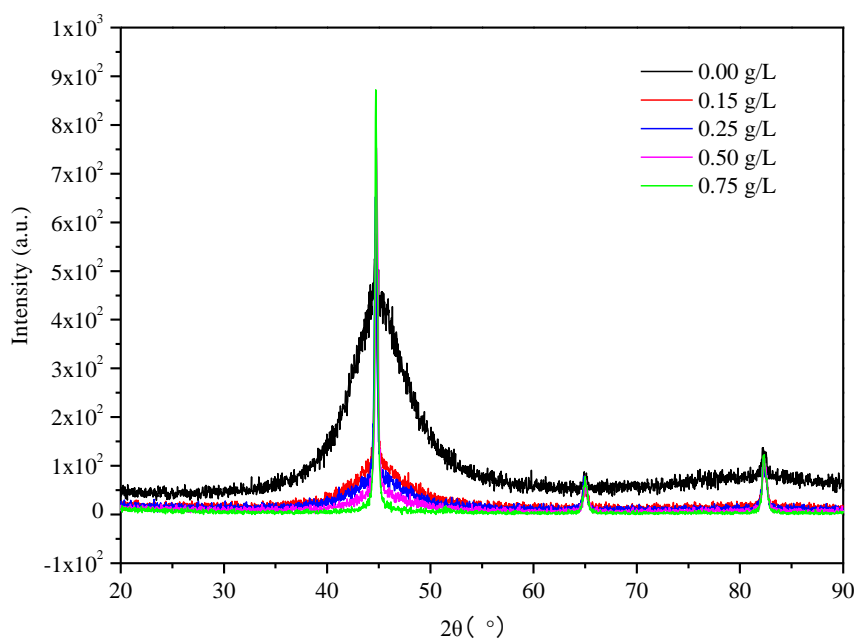


**Figure 4.** XRD pattern of electroless Ni-P-La coating under different concentration of  $\text{La}^{3+}$ : 0.00 g/L, 0.15 g/L, 0.25 g/L, 0.50 g/L, 0.75 g/L

The depth of P-containing coating reflects the thickness of the alloy layer. As shown in Figure 5, the phosphorus content of the coatings are substantially the same (7%), the thickness and the deposition rate of the coatings are different under different concentrations of La (0.15 g/L, 0.25 g/L, 0.5 g/L). The thickness of the coating decreases with the amount increase of La. That is to say, the increase of the rare earth elements (La) has a poor effect on the deposition rate. While for the coating quality, rare earth elements improve mainly the deposition state compared with the binary plating coating. The phosphorus (P) content of the coating stays the same, which indicates that the composition of the coating is consistent with the binary plating coating to some extent. Due to the conclusiveness of the structure and morphology of general materials to the performance of them, less addition amount of rare earth element (La) can optimize further the structure and morphology of the coating and make a contribution to the improvement of the coating properties correspondingly.

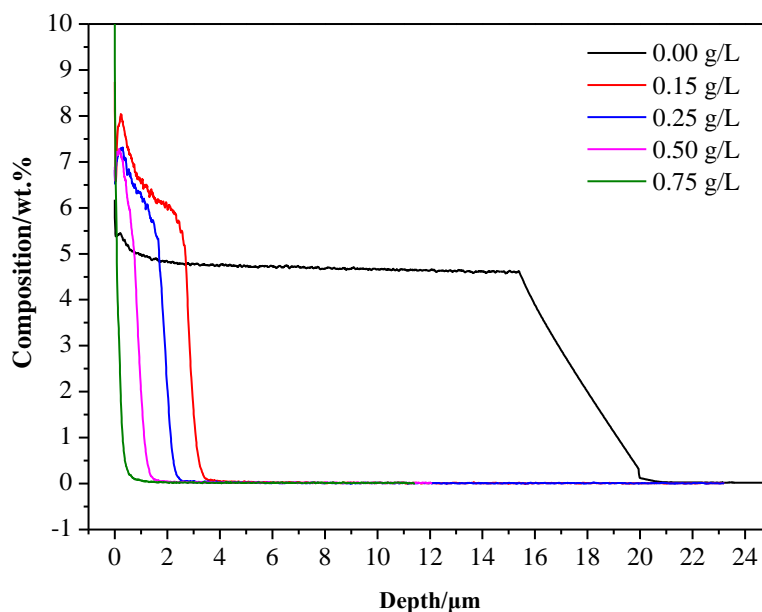


**Figure 5.** The P composition in Ni-P coatings under different concentration of  $\text{La}^{3+}$ : 0.00 g/L, 0.15 g/L, 0.25 g/L, 0.50 g/L, 0.75 g/L

### 3.2 Surface hardness

Figure 6, the bar chart showing the micro-hardness values under different addition amount of  $\text{La}^{3+}$ , which indicates that the hardness values is higher when the concentration of  $\text{La}^{3+}$  is in the range of 0.15-0.5 g / L. Rare earth element ( $\text{La}^{3+}$ ) with larger atomic size will be brought into the coating during the electroless plating process, which will produce certain lattice distortion in the coating and the spherical polarized structures containing certain atoms outside the rare earth atoms. With the increase of  $\text{La}^{3+}$ , polarization is enhanced and force, stress field between the atoms and the degree of lattice distortion are increased. So the resistance to dislocation motion is greatly improved for the plastic deformation under certain loading and the hardness is significantly increased. When the  $\text{La}^{3+}$

increases to a certain value, the hardness values decrease significantly, which indicate that the rare indeed improved the hardness of coating but the addition amount of it should be controlled strictly.

According to Hall-Pech theory[16], the hardness of the coating will increase with refining of the crystal grain. Based on the dislocation accumulation theory of nanocrystals and polycrystalline, the relationship between yield stress (hardness) and grain size can be expressed as:

$$\sigma = \sigma_0 + KH \cdot d^{-n} \dots\dots\dots (1)$$

$\sigma$ — macroscopic yield stress;  $\sigma_0$ —the lattice friction for the transfer of single dislocation; KH—a constant; d—the average grain diameter; n—the index of the average grain size, usually -1/2. However, this relationship is limit. First, the intensity will not grow indefinitely beyond theory. Secondly, any relaxation process on the grain boundaries may lead to the reduction of hardness, so the inverse HP phenomenon will appears at a critical grain size. Thirdly, HP theory base on the dislocation accumulation theory, so it is invalid for the ultrafine particles that may not produce a plurality of dislocation accumulation. And the displacement of the free grain boundaries may produce micro-cracks[17]. It also explains the phenomenon the most fine-grained Ni-P-La coatings under 0.5 g/L La<sup>3+</sup> show the lower hardness.

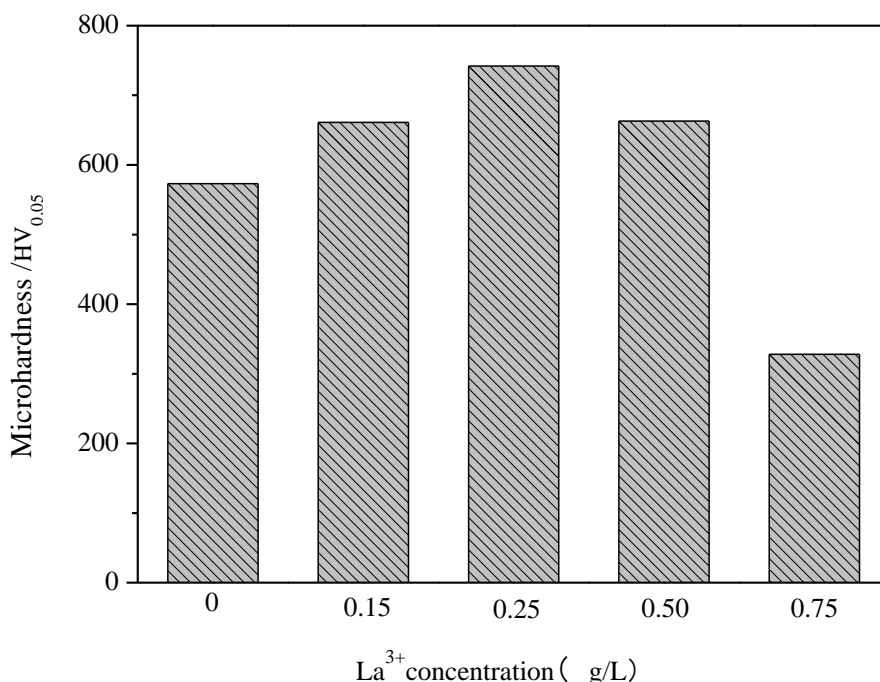


**Figure 6.** The microhardness bar chart of Ni-P coating under different concentration of La<sup>3+</sup>:0.15 g/L, 0.25 g/L, 0.50 g/L, 0.75 g/L

### 3.3 Tribological behaviors

The wear resistance performance of the coatings containing different La was tested by the reciprocating wear test under 5 N. The Ni-P coatings make the friction coefficient of substrate decreased from 0.711 to 0.467 under 5 N.

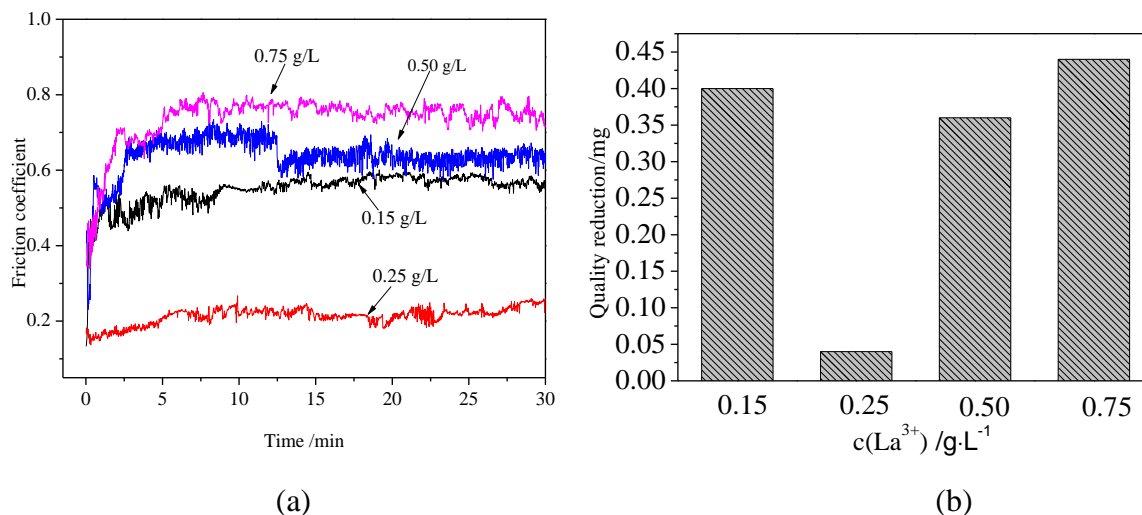


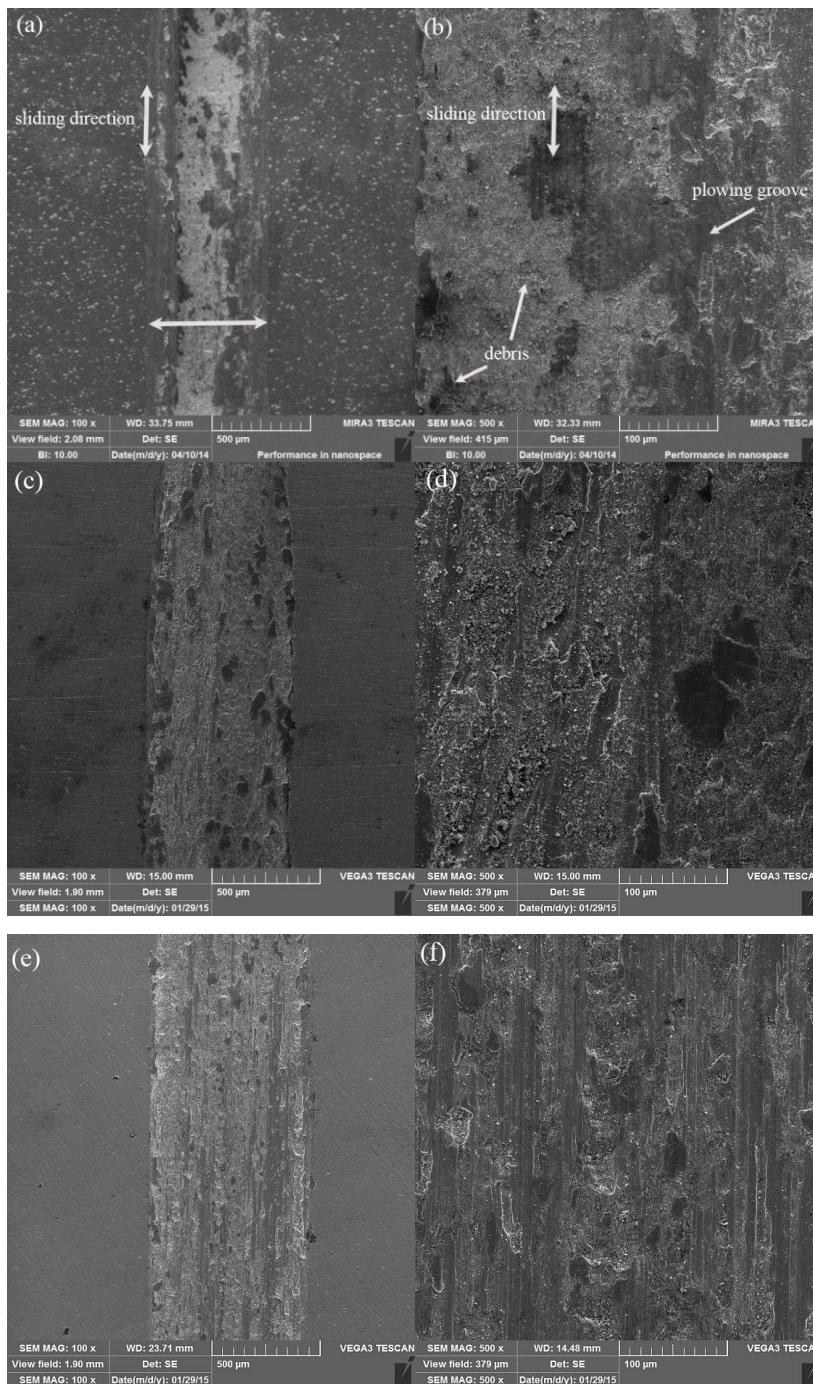
**Figure 7.** The friction coefficient curve (a) and mass loss bar chart (b) of Ni-P coating under different concentration of  $\text{La}^{3+}$  (0.15 g/L, 0.25 g/L, 0.50 g/L, 0.75 g/L) and a load of 5 N

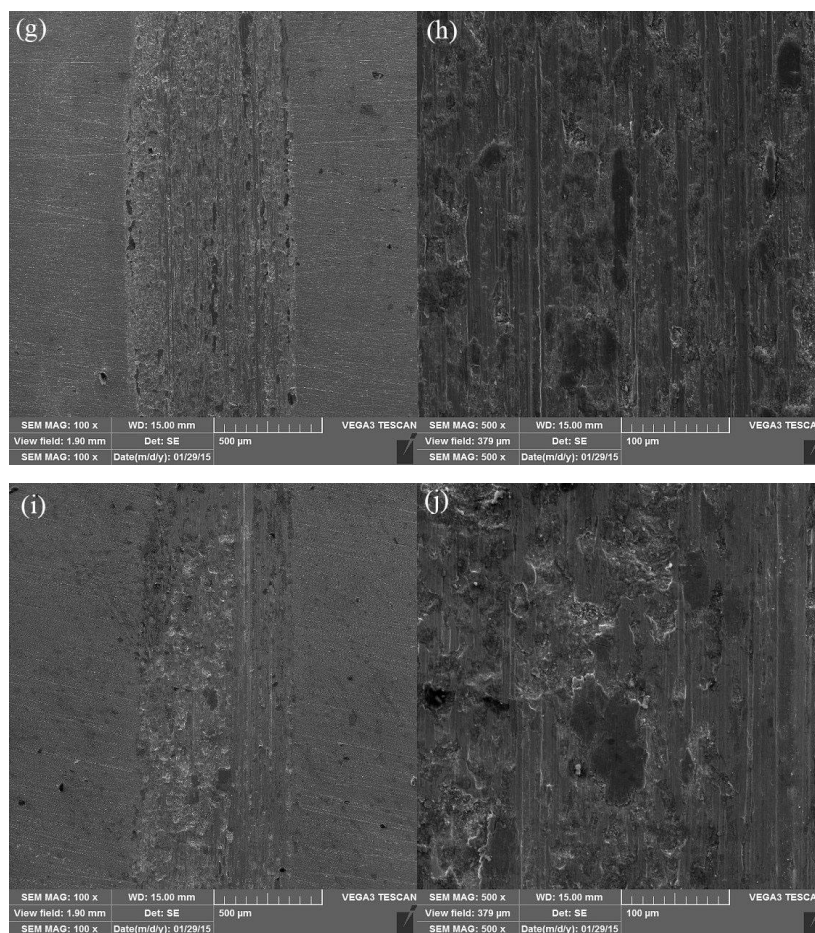
When the concentration of  $\text{La}^{3+}$  is 0.25 g / L, the coating surface is bright and smooth and the friction coefficient is significantly lower, the wear scar is shallower and the degree of wear is slighter than other coatings. In the wear test process, there is not sharp noise for those coatings which is also different from other coatings.

Figure 7a shows that the total friction coefficient increase continually with the increase of the concentration of  $\text{La}^{3+}$ . After a short running-in stage, wear process go into the stable wear stage. When the concentration of  $\text{La}^{3+}$  is 0.25 g / L, average friction coefficient of Ni-P-La alloy coatings is the minimum. And Figure 7b shows that the quality reduction of the coatings is also the minimum. Compared with the average friction coefficient (0.467) of Ni-P coatings under 5 N,  $\text{La}^{3+}$  do not significantly affect the average friction coefficient alloy coatings. Overall the coatings exhibit good wear resistance.

Seen from the electron microscope image (Figure 8) of the wear scars topography, there is no big difference between the widths of the wear scars on the different coatings containing different  $\text{La}^{3+}$ . There is obvious furrows on the surface wear scars of the coatings containing different  $\text{La}^{3+}$  content (0.25 g/L , 0.50 g/L , 0.75 g/L). When the concentration of  $\text{La}^{3+}$  is 0.25 g / L, the surface of the coating is bright, the furrows are thin and uniform and there are traces of the falling of some debris. When the concentration of  $\text{La}^{3+}$  is 0.50 g / L, the furrows are deeper and the coating surface is damaged severely. When the concentration of  $\text{La}^{3+}$  is 0.75 g / L, the furrows did not change much and the amount of wear debris reduces correspondingly compared with the coatings containing  $\text{La}^{3+}$  0.50 g / L. While there are pits leaved by the flaking of a large number of particles and the degree of wear is more serious compared with the two former. When the concentration of  $\text{La}^{3+}$  is 0.15 g / L, there are not significant furrows on the wear surface, but the wear morphology of the coating is close to the wear morphology of the substrate. The wear degree of the coatings is related with the thickness and hardness of them. Coatings with lower hardness exhibit the weaker resistance to wear. During the reciprocating

wear process, the effect of the abrasive falling on the coatings is smaller. The wear mechanism is adhesive wear, so there is a lot of wear debris existing on the wear surface. Overall, the effect of the addition of rare earth (La) had little effect on the wear properties of the coatings, which may be related with the structure and the hardness of the Ni-P alloy coatings[18, 19].





**Figure 8.** SEM images of worn surface morphologies on Ni-P coatings under different concentration of  $\text{La}^{3+}$  and a load of 5 N (left: 100X; right: 500X) (a, b) 0.00 g/L; (c, d) 0.15 g/L; (e, f) 0.25 g/L; (g, h) 0.50 g/L; (i, j) 0.75 g/L

### 3.4 Corrosion resistance

The polarization curves (Figure 9) of different coatings under the condition of 5 wt.% NaCl and ambient temperature show that the corrosion potential shift positively, the corrosion current density decrease and the corrosion resistance of the coating improve with the increase of La content when the content of  $\text{La}^{3+}$  is less than 0.50 g / L (Table 4). When the content of  $\text{La}^{3+}$  is 0.15 g/L, a certain passivation area emerges in the anode branch and the coatings exhibit a good corrosion resistance. When the content of  $\text{La}^{3+}$  is 0.50 g/L, the corrosion potential of the coating achieve to the highest, the corrosion current density is the minimum and the overall corrosion resistance of the coating is the optimum. Conversely, when the content of  $\text{La}^{3+}$  is increased to 0.75 g/L, the corrosion potential shift negatively in a greater degree and the current density will also increase accordingly. Besides Tafel slopes  $\beta_a$  and  $\beta_c$  also inversely impact the corrosion current density and the result is consistent with the above results.

These show that the passivation of the coating is weaker and the stability of it is also greatly reduced, which is mainly due to the reduction of the coating quality. The change of the surface morphology caused by rare earth (La) induce the change of corrosion resistance of the coating

accordingly[20, 21]. The coatings formed under appropriate addition of La indicated the following characteristics: 1) The cell structure of them is compact and smooth; 2) the potential difference between the central raised portion and the edge portion is small; 3) the fluctuation of the components is smaller than that of the traditional coatings with coarse cell particles; 4) the distribution of the phosphorus content in micro area is also uniform. The tendency of electrochemical corrosion is reduced and the corrosion resistance is improved and enhanced[15, 20].

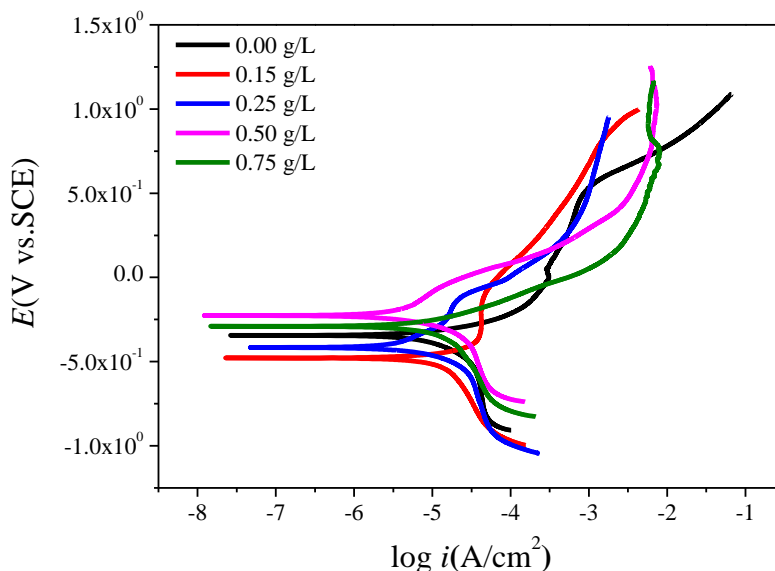


**Figure 9.** Polarization curves of Ni-P-La coatings deposited in different La-added plating solution (0.00 g/L, 0.15 g/L, 0.25 g/L, 0.50 g/L, 0.75 g/L) in 5 wt.% NaCl

**Table 4.** The data of electrochemical polarization curves of Ni-P-La coatings deposited in different La-added plating solution(0.00 g/L, 0.15 g/L, 0.25 g/L, 0.50 g/L, 0.75 g/L) in 5 wt.% NaCl

Samples	$E_{corr}$ (V vs.SCE)	$I_{corr}$ ( $\mu\text{A}/\text{cm}^2$ )	$\beta_a$ (V/decade)	$\beta_c$ (V/decade)
Ni-P coating	-0.393	6.026	0.058	0.127
0.15 g/L	-0.478	4.335	0.065	0.145
0.25 g/L	-0.417	2.741	0.114	0.146
0.50 g/L	-0.227	0.843	0.171	0.168
0.75 g/L	-0.290	6.516	0.106	0.074

Seeing from the electrochemical impedance Nyquist plot (Figure 10) of different Ni-P plating coating containing La, all the curves are composed of a single semicircle in the high frequency region. That is to say the common electrochemical reaction is a process of transferring and controlling electric charge and there is a time constant in the process of etching for coating. However, the different semicircle radius indicates that the effective areas of reaction processes under different conditions are different and the corrosion resistance of the coatings is different.

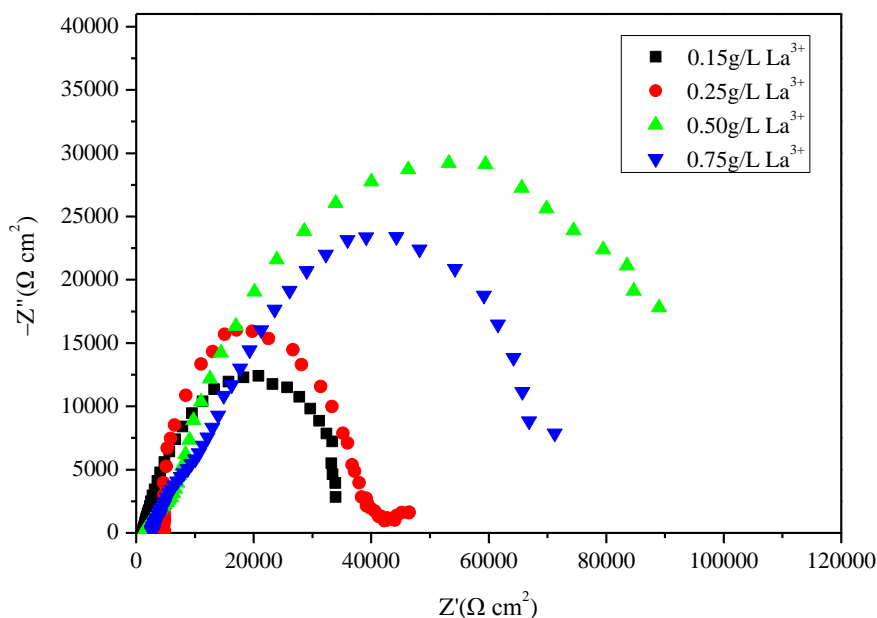


**Figure 10.** Electrochemical Nyquist plot of Ni-P-La coatings deposited in different La-added plating solution (0.15 g/L, 0.25 g/L, 0.50 g/L, 0.75 g/L) in 5 wt.% NaCl

The corrosion behavior of the coatings is further compared and analyzed through the fitting of equivalent circuit model (Figure 11). The equivalent circuit includes five components:  $R_1$ —the resistance of solution;  $Q$ —the capacitance of the interface of coating/solution;  $R_2$ —the resistance of the interface of coating/solution;  $C$ —electric double-layer capacitance of the interface of coating/substrate;  $R_3$ —the charge transfer resistance of the interface of coating/substrate. Among them the  $Q$  is a constant phase element (CPE) used to describe the deviation between  $C$  and the ideal capacitance[21].

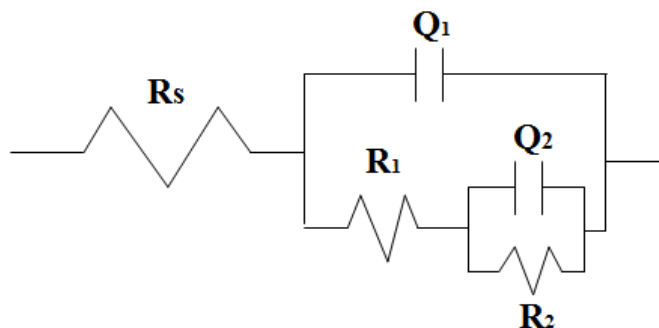


**Figure 11.** Equivalent electrical circuit model used to analyze the EIS data of Ni-P coatings under different adding content of rare earth

The corresponding parameters are shown in Table 5. The  $R_{ct}$  of the Ni-P coatings containing La is higher significantly than that of the Ni-P coatings ( $3279 \Omega \cdot \text{cm}^2$ ). And the  $n$  characterizes the

degree of the deviation between C and the ideal capacitance. The value of n is smaller, the deviation is bigger. Besides, the value of  $R_1$  and Q change slightly, which reflect the nature of the solution environment and the coating itself are consistent. While the charge transfer resistance of two interface ( $R_2+R_3$ ) is different. When the addition amount of La is 0.50 g/L, the resistance value between the solution and the substrate is maximum. In another words, the corrosion resistance of the coating is the optimal. This result is consistent with the analysis of the polarization curves.

**Table 5.** The impedance date of plated Ni-P coating under different addition amount of La: 0.15 g/L, 0.25 g/L, 0.50 g/L, 0.75 g/L)

Samples	$R_s(\Omega \cdot \text{cm}^2)$	$Q_1(\text{F}/\text{cm}^2)$	$R_1(\Omega \cdot \text{cm}^2)$	$Q_2(\text{F}/\text{cm}^2)$	$R_2(\Omega \cdot \text{cm}^2)$	$R_{ct}(\Omega \cdot \text{cm}^2)$
Ni-P-0.15 g/L	94.33	1.36E-4	4505	3.45E-4	3764	8269
Ni-P-0.25 g/L	93.64	1.10E-4	6248	2.93E-4	4367	10615
Ni-P-0.50 g/L	92.17	2.11E-4	7719	1.41 E-4	6348	14067
Ni-P-0.75 g/L	97.97	3.87E-4	9572	4.05 E-4	1722	11294

#### 4. CONCLUSIONS

This work shows that La has positively affect the modification of the Ni-P coatings on the anchor rod material (RB400). According to the experiment we can draw the following conclusions:

- 1) The effect of  $\text{La}^{3+}$  on the surface morphology of the Ni-P plating coating is significant. The surface cellular particles of the coating are refined and the arrangement of them is more compact. When the addition amount of  $\text{La}^{3+}$  is 0.50 g / L, the coating surface is very smooth and the compact degree of cellular particles is the best.
- 2) The FWHM of the peaks for the coatings containing La has been narrowed and show significant features of microcrystalline diffraction and the XRD pattern of the coatings containing La present fewer small peak.
- 3)  $\text{La}^{3+}$  indeed improved the hardness of coating but the addition amount of it should be controlled strictly. The hardness values of the Ni-P alloy coatings are higher when the concentration of  $\text{La}^{3+}$  concentration is in the range of 0.15-0.5 g/L.
- 4) The total friction coefficient increase continually with the increase of content of the  $\text{La}^{3+}$ . When the concentration of  $\text{La}^{3+}$  is 0.25 g/L, average friction coefficient of Ni-P-La alloy coatings is the lowest, the wear scar is the shallowest and the degree of wear is the slightest. While compared with that of Ni-P coatings,  $\text{La}^{3+}$  do not significantly affect the average friction coefficient of alloy coatings.
- 5) With the increase of  $\text{La}^{3+}$ , the corrosion resistance of the coatings increase firstly and then decrease. When the content of  $\text{La}^{3+}$  is 0.50 g/L, the corrosion potential of the coating is the highest, the corrosion current density is the minimum and the overall corrosion resistance of the coating is the optimum.

However, the action mechanism of La about the corrosion resistance is not yet clear and it will be the object of study in the future.

#### ACKNOWLEDGEMENTS

This work was supported by the National Natural Science Foundation of China (No. 51501125), the China Postdoctoral Science Foundation (No.2012M520604), the Natural Science Foundation for Young Scientists of Shanxi Province (No.2013021013-2, No.2014011036-1 No.2014011015-7) the Science and Technology Programs for Research and Development of Shaanxi Province (No. 2013KJXX-08).

#### References

1. N.M. Lin, H.Y. Zhang, J.J. Zou, P.J. Han, Y. Ma and B. Tang. *Int. J. Electrochem. Sci.*, 10 (2015) 356-372.
2. O. Elendu, M. Ojewumi, Y.D. Yeboah and E.E. Kalu. *Int. J. Electrochem. Sci.*, 10 (2015) 10792-10805.
3. C.O. Osifuye, A.P.I. Popoola, C.A. Loto and D.T. Oloruntoba. *Int. J. Electrochem. Sci.*, 9 (2014) 6074-6087.
4. R.X. Sun, Zhao, G. Yu, Z.H. Xie, B.N. Hu, J. Zhang, X.M. He and X.Y. Zhang. *Int. J. Electrochem. Sci.*, 10 (2015) 7893-7904.
5. A. Małeckı and A. Micek-Ilnicka. *Surf. Coat. Technol.*, 123 (2000) 72-77.
6. J.H. Wang, X.M. Fei, G.D. Long and W. Li. *Mater. Prot.*, 36 (2003) 31-33.
7. J.Z. Li, Y.W. Tian, Y. Li and X. Wang. *J. Rare Earths*, 28 (2010) 769-773.
8. H. Ashassi-Sorkhabi, M. Moradi-Haghighi and M.G. Hosseini. *Surf. Coat. Technol.*, 202 (2008) 1615-1620.
9. Y. Zhu, L. You and T.T. Song. *Plat. Finish.*, 30 (2011) 20-22.
10. J.N. Balaraju and M. Chembath. *Appl. Surf. Sci.*, 258 (2012) 9692-9700.
11. H.M. Jin, S.H. Jiang and L.N. Zhang. *J. Rare Earths*, 27 (2009) 109-113.
12. X.W. Zhou, Y.F. Shen and H.M. Jin. *Funct. Mater.*, 42 (2011) 305-309.
13. Z.H. Ren and L.P. Tian. *China Surf. Eng.*, 25 (2012) 79-83.
14. B. Szczygieł, A. Turkiewicz and J. Serafińczuk. *Surf. Coat. Technol.*, 202 (2008) 1904-1910.
15. H. Sun, H.F. Ma, X.F. Guo, L.M. Feng, Y. Wang and Y.X. Cai. *J. Chin. Soc. Rare Earths*, 32 (2014) 228-233.
16. Z.X. Zou, J.Z. Xiang and S.Y. Xu. *Trans. Mater. Heat Treat.*, 35(2014) 137-141.
17. D. Wang, Y.F. Cheng, H.M. Jin, J.Q. Zhang and J.Q. Gao. *J. Rare Earths*, 31 (2013) 209-214.
18. Y.H. Ma, Q.H. Zhang and Y.Z. Li. *J. Electrochem. Soc.*, 159 (2012) D119-D123.
19. F. Mo, Y. Feng, Y.M. Chen, Y.Q. Wang, G. Qian, Y.K. Dou and X.B. Zhang. *J. Rare Earths*, 33 (2015) 327-333.
20. L. Jiang, J. B. Lu, S.S. Pan, Y.D. Yu, G.Y. Wei and H.L. Ge. *Int. J. Electrochem. Sci.*, 7 (2012) 2188-2200.
21. A.S. Hamdy and H.M. Hussien. *Int. J. Electrochem. Sci.*, 8 (2013) 11386-11402.